University of Reading

Bond-graph Input-State-Output Port-Hamiltonian formulation of memristive networks for emulation of Josephson junction circuits

Article

Published Version

It is advisable to refer to the publisher's version if you intend to cite from the work. See Guidance on citing.

www.reading.ac.uk/centaur

CentAUR

Central Archive at the University of Reading

Reading's research outputs online

PAPER • OPEN ACCESS

Bond-Graph Input-State-Output Port-Hamiltonian Formulation of Memristive Networks for emulation of Josephson Junction Circuits

IOP ebooks™

Bringing you innovative digital publishing with leading voices to create your essential collection of books in STEM research.

Start exploring the collection - download the first chapter of every title for free.

Bond- Graph Input-State-Output Port-Hamiltonian Formulation of Memristive Networks for emulation of Josephson Junction Circuits

Israa Badr Nasser Al-Mashhadani[1] and Sillas Hadjiloucas[2]

[1]College of Engineering, Computer Engineering Department, Al-Nahrain University, Baghdad, Iraq
[2]Biomedical Engineering Department, University of Reading, RG6 6AY, UK

Correspondance emails : i.b.al-mashhadani@eng.nahrainuniv.edu.iq; s.hadjiloucas@reading.ac.uk

Abstract. A bond graph Input-State-Output Port-Hamiltonian formulation of memristive networks for Josephson junction circuits in state space is presented. The methodology has applications to the modeling of SQUIDs and other non-linear transducers and enables the formulation of input-output models of complex components embedded in non-linear networks.

1. Introduction

As suggested first by Paynter in 1959 [3], circuits that consist of non-linear elements can be analysed using Bond graph (BG) modelling. Following his work, in the 70's Oster [2] proposed to integrate the memristor with the other bond graph elements [3, 4]. The method provides a graphical representation of a physical systems and is designed to represent the continuous flow of the power or the energy exchanges within the components of a system using energy and power alone. This type of modeling can incorporate processes in multiple domains seamlessly (e.g. mechanical, electrical, magnetic, etc.).

Because of the non-linearity associated to the response of memristive components, Laplace transforms may not be used to derive transfer functions that would uniquely relate the input with the output function of these 2-port devices. Their dynamics may be studied instead, using differential algebraic models arising from descriptor representations derived from nodal analysis associated to the underlying circuit topology. Since circuits with memristive components interact nonlinearly, in order to formulate a BG model of a circuit, one needs to consider two dissipative parts, a linear one for the resistive behaviour (R) and a nonlinear one for the memristive behaviour (M).

State space models of the circuit dynamics are made possible by adopting an Input-State-Output Port-Hamiltonian System (ISO-PHS), directly from bond-graph analysis. In our previous work [5] it was shown that the equations obtained from BG can be mapped to Port-Hamiltonian System (PHS) formulations [6, 7]. PHS formulations preserve the energy exchange between storage, dissipation, source and junction structures. Both PHS and BG representations share the same fundamental postulations making inter-conversion between the two formulations possible. Memristors have also been discussed within a port-Hamiltonian framework by Jeltsema [8, 9].

2. Bond graph with nonlinear elements

In BG theory, power is the result of the product between effort $e(t)$ and flow $f(t)$. Flow and effort variables at all the ports of the network are described using causality postulations. The causality concept is used to assign the direction of power-conjugated input-output pairs [10]. As discussed in [11], a BG general structure is composed of: dissipation fields that can be splits into two parts (linear and nonlinear), storage fields (C and I), source fields associated with effort and flow (S_e and S_f), and junction structures (denoted by JS) containing transformers TF and gyrators GY as shown in Fig. 1. Dissipation is seen as composed of input (subscript i) and output variables (subscript o). The dissipation variables consist of two types of elements: linear (superscript l) and nonlinear (memristive behaviour with superscript M). Similar expressions can be defined to model memristive dissipative elements using the BG framework after assuming the following general junction structure in Fig. 1:
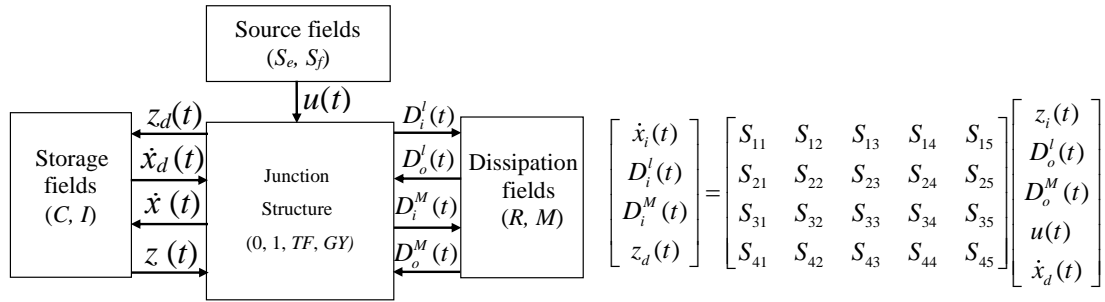
Fig. 1 Structure of a causal bond graph and corresponding state space matrix representation.

A defined junction structure for systems with a memristor can be developed using the generic expression shown in Fig. 1 after making the following hypotheses: (a) All storage elements are linear, (b) all storages are in integral causality (which implies there is no element in differential causality) this leads to $S_{41} = S_{15} = 0$, (c) no storages are assigned in differential causality by source $(S_{44} = 0)$, (d) by definition the dependent state variables are functions only of integral causal state and the system inputs $(S_{42} = S_{45} = S_{43} = 0)$, (e) in the case where there are no coupled resistors $(S_{22} = S_{32} = S_{23} = S_{33} = 0)$.

In the derivation for a system with linear storage elements and non-linear dissipative elements, the constitutive relations of the elements are defined as follows: $z(t) = Fx(t)$, $x_d(t) = Gz_d(t)$, $D_o^I(t) = LD_i^I$, $D_o^M(t) = M(x)D_i^M(t)$ where $x(t)$ is an integral causal input variable, $x_d(t)$ is a differential causal input variable and u are the output variables. Substituting these constitutive relations into the ones in Fig 1:

$$\begin{bmatrix} \dot{x}_i(t) \\ D_i^I(t) \\ D_i^M(t) \\ z_d(t) \end{bmatrix} = \begin{bmatrix} S_{11}F & S_{12}L & S_{13}M & S_{14} & S_{15}G \\ S_{21}F & S_{22}L & 0 & S_{24} & 0 \\ S_{31}F & 0 & 0 & S_{34} & 0 \\ S_{41}F & 0 & 0 & 0 & 0 \end{bmatrix} \begin{bmatrix} x_i(t) \\ D_i^I(t) \\ D_i^M(t) \\ u(t) \\ \dot{z}_d(t) \end{bmatrix} \tag{1}$$

which leads to:

$$\dot{x}(t)E = \left[S_{11} + S_{12}L(I - S_{22}L)^{-1}S_{21} + S_{13}M(x)S_{31} \right]Fx(t) + \left[S_{12}L(I - S_{22}L)^{-1}S_{24} + S_{13}M(x)S_{34} + S_{14} \right]u(t) \tag{2}$$

where $E = (I - S_{15}GS_{41}F)$. This is a state space equation of the form $\dot{x}(t) = Ax(t) + Bu(t)$. It is worth noting that the above expression is still not a proper PHS formulation. This is discussed in the following section.

3. ISO-PHS Formulation

A Port-Hamiltonian framework incorporates the interconnection structure of power dissipation within the system. The total energy flow expressions across ports reflect the circuit physical structure using a Hamiltonian function $H(x)$. Thus, Port-Hamiltonian systems (PHS) have a physical interpretation associated with connectivity of all the elements in the circuit.

One important class of PHS is the standard ISO-PHS formulation. In this formulation, the *flow* and *effort* variables are split into input-output pairs of power-conjugated charge and momentum (q, p) [12]. The generic input state-output port-Hamiltonian for the total stored energy is:

$$\dot{x} = \left[J(x) - R(x) \right] \frac{\partial H}{\partial x}(x) + g(x)u, \qquad y = g^T(x)\frac{\partial H}{\partial x}(x) \tag{3}$$

where $H(q, p)$ represents the total energy stored in the system for the conjugate variables, x is the state variable, u and y are the power variables of the input and output ports, $g(x)$ is the output vector, $J(x)$ is a skew-symmetric matrix representing the interconnection structure (which is power conserving), and $R(x)$ is the dissipation structure symmetry matrix. The skew-symmetric properties in $J(x)$ imply that the flow of energy within the circuit is such that the power consumed by the inductors and the capacitors equals the difference between the power provided to the circuit by the external port and the power dissipated by the resistors.

To compute $H(x)$ using BG variables, first the energy function $E(x)$ must be expressed as the integration of power which is the product between the input and output variables of the storage elements [13].

$$E(x_i, x_d) = \int z_i^T x_i \partial t + \int z_d^T x_d \partial t \tag{4}$$

One can write:.

$$E(x_i, x_d) = E(x_i, g(z_d)) = E(x_i, g(s_{41}z_i)) = H(x_i) \tag{5}$$

The total energy $H(x)$ expressed using BG variables is:

$$\frac{\partial H}{\partial x} = \left[I - FS_{15}GS_{41} \right] z_i \tag{6}$$

Substituting (6) into (2), the resulted equation will be:

$$\dot{x}(t) = E^{-1} \left[S_{11} + \underbrace{S_{12}L(I - S_{22}L)^{-1}S_{21}}_{W} + \underbrace{S_{13}M(x)S_{31}}_{W_M} \right](I - FS_{15}GS_{41})^{-1}\frac{\partial H}{\partial x}$$
$$+ E^{-1} \left[S_{12}L(I - S_{22}L)^{-1}S_{24} + S_{13}M(x)S_{34} + S_{14} \right]u(t) \tag{7}$$

From the definition of J it can be observed that this is a skew-symmetric matrix, where $J=-J$. Similarly, R is a symmetric matrix. The expressions of symmetric and skew-symmetric components are defined in terms of BG as follows:

$$E^T = (I - FS_{15}GS_{41})^{-1} \tag{8}$$

$$W = S_{12}L(I - S_{22}L)^{-1}S_{21} \tag{9}$$

$$W_{sy} = \frac{1}{2} \left[S_{12}L(I - S_{22}L)^{-1}S_{21} + \left[S_{12}L(I - S_{22}L)^{-1}S_{21} \right]^T \right] \tag{10}$$

$$W_{sk} = \frac{1}{2} \left[S_{12}L(I - S_{22}L)^{-1}S_{21} - \left[S_{12}L(I - S_{22}L)^{-1}S_{21} \right]^T \right] \tag{11}$$

where W_{sy} and W_{sk} are the symmetric and skew-symmetric parts of (7). For the expression in Eq. (7) that contains the memristance M, the symmetric and skew-symmetric parts are:

$$W_M = S_{13}M(x)S_{31} \tag{12}$$

$$W_{M,sy} = \frac{1}{2}\left[S_{13}M(x)S_{31} + \left[S_{13}M(x)S_{31}\right]^T\right],\tag{13}$$

$$W_{M,sk} = \frac{1}{2}\left[S_{13}M(x)S_{31} - \left[S_{13}M(x)S_{31}\right]^T\right]\tag{14}$$

As $J(x)$ combines the skew-symmetric parts of Eqs 11 and14 and $R(x)$ combines the symmetric parts of Eqs 10 and 13, it follows that the system equation matrices shown in (3) will be:

$$J(x) = E^T S_{11} E + E^T W_{sk} E + E^T W_{M,sk} E\tag{15}$$

$$R(x) = -E^T W_{sy} E + E^T W_{M,sy} E\tag{16}$$

$$g(x) = E^T\left[S_{12}L(I - S_{22}L)^{-1}S_{24} + S_{13}M(x)S_{34} + S_{14}\right]\tag{17}$$

4. Formulating PCHD models of sensor systems using bond graphs: A Josephson junction application example:

Josephson junctions circuits can be broadly defines as circuit components where there is a flow of current and voltage across a weak link when there is quantized current leakage even in the absence of a constant source supply [14]. Such junctions have important applications in quantum-mechanical circuits e.g. in magnetic sensors where they can measure the total magnetic field or the vector components of the magnetic field [15]. An important class of sensing elements that make use of the Josephson junction current to perform measurements are the superconducting quantum interference devices (SQUIDs). In their simplest realisation these have two Josephson junctions in parallel in a superconducting loop [16]. An electrical model of a Josephson junction using memristive elements is shown in Fig. 2a. [17].
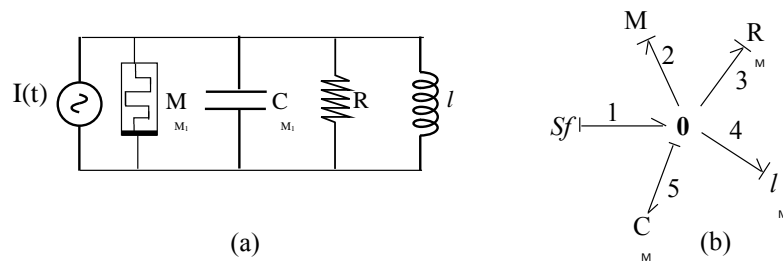

Fig. 2 (a) Josephson junction circuit model with the non-linearity emulated using a memristor.
(b) The corresponding bond graph with causality marks.

The corresponding bond graph for the circuit in preferential integral causality is shown in fig.2b. It can be seen that there are no internal connections, and the derived junction structure matrix after rearranging the junction elements into the form of Eq. (2) is:

$$\begin{bmatrix} e_4 \\ f \\ e_3 \\ e_2 \end{bmatrix} = \begin{bmatrix} 0 & 1 & 0 & 0 & 0 & 0 \\ -1 & 0 & -1 & -1 & 1 & 0 \\ 0 & 1 & 0 & 0 & 0 & 0 \\ 0 & 1 & 0 & 0 & 0 & 0 \\ 0 & 0 & 0 & 0 & 0 & 0 \end{bmatrix} \begin{bmatrix} f_4 \\ e_5 \\ f_3 \\ f_2 \\ f_1 \end{bmatrix}\tag{18}$$

The constitutive relations are: $F_1 = \frac{1}{l}$, $F_2 = \frac{1}{C}$, $L = \frac{1}{R}$, $M = \frac{1}{M(\phi)}$. The ISO PH matrices for a

Josephson junction circuit can be expressed by using equations (7-13) as follows:

$$k_d = I, \quad k_d^T = I, \quad W = \begin{bmatrix} 0 & 0 \\ 0 & -\dfrac{1}{R} \end{bmatrix}, \quad W_{sy} = \begin{bmatrix} 0 & 0 \\ 0 & -\dfrac{1}{R} \end{bmatrix}, \quad W_{sk} = \begin{bmatrix} 0 & 0 \\ 0 & 0 \end{bmatrix}, \quad W_M = \begin{bmatrix} 0 & 0 \\ 0 & -\dfrac{1}{M(\phi)} \end{bmatrix},$$

$$W_{M,sy} = \begin{bmatrix} 0 & 0 \\ 0 & -\dfrac{1}{M(\phi)} \end{bmatrix}, \quad W_{M,sk} = \begin{bmatrix} 0 & 0 \\ 0 & 0 \end{bmatrix}$$

From the above matrices, it is possible to obtain the Port-Hamiltonian system components (1).

$$J = \begin{bmatrix} 0 & 1 \\ -1 & 0 \end{bmatrix}, \quad R = \begin{bmatrix} 0 & 0 \\ 0 & -\dfrac{1}{R} - \dfrac{1}{M(\phi)} \end{bmatrix}, \quad g = \begin{bmatrix} 0 \\ 1 \end{bmatrix}.$$

5. Conclusion

ISO-PHS formulations are derived from BG to model the memristive behaviour of a Josephson junction circuit and should enable the modelling of more complex networks associated to recently proposed SQUID designs. These have applications in the modelling of dielectric loading in HTS resonators [18][19] enabling them to be used for the implementation of phase conjugation in the microwave region [20]. Additional applications can be found in the modelling of noise in magnetic field measurements [21], in inductive measurements [22] also as applied to thermometry and calorimetry [23, 24], in single-photon and macro-molecule detection [25, 26], and other quantum detection sensing schemes as well as in nano-electromechanical systems e.g., resonators [27]. The formulations should be also particularly useful for the design of coupled nanoSQUIDs [28, 29] e.g., Dayem Bridge Junctions [30].

The methodology has also other applications to other sensors and transducers that have non-linear responses and are embedded in more complex networks as encountered in the modelling of bio-dielectrics e.g., neuronal structures [31]. The proposed analysis should also find new uses in the analysis of other RLCM networks, thus extending the applications of PHS-BG theory originally proposed by Donaire [13].

References

[1]   H. Paynter, *Analysis and design of engineering systems*. Cambridge: MIT press, 1961.
[2]   G. Oster and D. Auslander, "The memristor: a new bond graph element," *J. Dyn. Syst. Meas. Control*, vol. 94, no. 3, pp. 249–252, 1972.
[3]   L. Chua, "Memristor-The missing circuit element," *IEEE Trans. Circuit Theory*, vol. 18, no. 5, pp. 507–519, 1971.
[4]   D. Strukov, G. Snider, D. Stewart, and S. Williams, "The missing memristor found.," *Nature*, vol. 453, no. 7191, pp. 80–3, May 2008.
[5]   Al-Mashhadani, I. B. N. and Hadjiloucas, S. (2017) Port hamiltonian formulation of a memristive switch circuit represented in bond graph. In: 2017 IEEE SENSORS. ISBN 9781509010127
[6]   A. Van der Schaft, "Port-controlled Hamiltonian systems: towards a theory for control and design of nonlinear physical systems," *J. Soc. Instrum. Control Eng. Japan (SICE),* vol. 29, no. 2, pp. 91–98, 2000.
[7]   A. van der Schaft and D. Jeltsema, *Port-Hamiltonian Systems Theory: An Introductory Overview*. Hanover, USA: now Publishers Inc., 2014.
[8]   D. Jeltsema and A. Doria-Cerezo, "Port-Hamiltonian Formulation of Systems With Memory," *Proc. IEEE*, vol. 100, no. 6, pp. 1928–1937, Jun. 2012.
[9]   D. Jeltsema and A. van der Schaft, "Memristive port-Hamiltonian Systems," *Math. Comput. Model. Dyn. Syst.*, vol. 16, no. 2, pp. 75–93, May 2010.

[10] W. Borutzky, *Bond Graph Methodology: Development and Analysis of Multidisciplinary Dynamic System Models*, vol. 26. London, UK: Springer Science & Business Media, 2009.

[11] G. Avalos and R. Orozco, "A procedure to linearize a class of non-linear systems modelled by bond graphs," *Math. Comput. Model. Dyn. Syst.*, vol. 21, no. 1, pp. 38–57, Jan. 2014.

[12] G. Golo, A. van der Schaft, P. Breedveld, and B. Maschke, "Hamiltonian formulation of bond graphs," in *Nonlinear and Hybrid Systems in Automotive Control*, London, UK: Springer, 2003, pp. 351–372.

[13] A. Donaire and S. Junco, "Derivation of Input-State-Output Port-Hamiltonian Systems from bond graphs," *Simul. Model. Pract. Theory*, vol. 17, no. 1, pp. 137–151, Jan. 2009.

[14] B. Josephson, "Possible new effects in superconductive tunnelling," *Phys. Lett.*, vol. 1, no. 7, pp. 251–253, 1962.

[15] J. Lenz and S. Edelstein, "Magnetic sensors and their applications," *IEEE Sens. J.*, vol. 6, no. 3, pp. 631–649, Jun. 2006.

[16] D. Drung, C. Assmann, J. Beyer, A. Kirste, M. Peters, F. Ruede, and T. Schurig, "Highly Sensitive and Easy-to-Use SQUID Sensors," *IEEE Trans. Appl. Supercond.*, vol. 17, no. 2, pp. 699–704, Jun. 2007.

[17] L. Chua, "Nonlinear circuit foundations for nanodevices, part I: the four-element torus," *Proc. IEEE*, vol. 9, no. 11, pp. 1830–1859, Nov. 2003.

[18] L. Hao, J. Gallop, A. Purnell, L. Cohen, and S. Thiess, "Non-linear microwave response of HTS thin films: a comparison of intermodulation and conventional measurements," *IEEE Trans. Appiled Supercond.*, vol. 11, no. 1, pp. 3411–3414, Mar. 2001.

[19] J. Gallop, C. Langham, L. Hao, and F. Abbas, "Dielectric loaded HTS resonators as frequency standards and low-phase noise oscillators," *IEEE Trans. Instrum. Meas.*, vol. 46, no. 2, pp. 122–125, Apr. 1997.

[20] L. Hao, J. Gallop, and J. Macfarlane, "Applications of Superconductivity for Implementation of Phase Conjugation in the Microwave Region," *J. Supercond. Nov. Magn.*, vol. 19, no. 7–8, pp. 591–598, Feb. 2007.

[21] E. Romans, S. Rozhko, L. Young, A. Blois, L. Hao, D. Cox, and J. Gallop, "Noise Performance of Niobium Nano-SQUIDs in Applied Magnetic Fields," *IEEE Trans. Appl. Supercond.*, vol. 21, no. 3, pp. 404–407, Jun. 2011.

[22] L. Hao, J. Macfarlane, S. Lam, C. Foley, P. Josephs-Franks, and J. Gallop, "Inductive Sensor Based on Nano-Scale SQUIDs," *IEEE Trans. Appiled Supercond.*, vol. 15, no. 2, pp. 514–517, Jun. 2005.

[23] R. Lee, L. Hao, D. Peden, J. Gallop, J. Macfarlane, and E. Romans, "Quantum Roulette Noise Thermometer: Progress and prospects," *IEEE Trans. Appiled Supercond.*, vol. 11, no. 1, pp. 859–862, Mar. 2001.

[24] J. Gallop, D. Cox, and L. Hao, "Nanobridge SQUIDs as calorimetric inductive particle detectors," *Supercond. Sci. Technol.*, vol. 28, no. 8, p. 84002, Aug. 2015.

[25] A. Watson, "Measurement and the single particle.," *Science*, vol. 306, no. 5700, pp. 1308–9, Nov. 2004.

[26] L. Hao, J. Gallop, C. Gardiner, P. Josephs-Franks, J. Macfarlane, S. Lam, and C. Foley, "Inductive superconducting transition-edge detector for single-photon and macro-molecule detection," *Supercond. Sci. Technol.*, vol. 16, no. 12, pp. 1479–1482, Dec. 2003.

[27] L. Hao, "Quantum Detection Applications of NanoSQUIDs fabricated by Focussed Ion Beam," *J. Phys. Conf. Ser.*, vol. 286, no. 1, p. 12013, Mar. 2011.

[28] L. Hao, D. Cox, J. Gallop, J. Chen, S. Rozhko, A. Blois, and E. Romans, "Coupled NanoSQUIDs and Nano-Electromechanical Systems (NEMS) Resonators," *IEEE Trans. Appl. Supercond.*, vol. 23, no. 3, pp. 1800304–1800304, Jun. 2013.

[29] S. Bechstein, F. Ruede, D. Drung, J. Storm, C. Kohn, O. Kieler, J. Kohlmann, T. Weimann, T. Patel, B. Li, D. Cox, J. Gallop, L. Hao, and T. Schurig, "Design and Fabrication of Coupled NanoSQUIDs and NEMS," *IEEE Trans. Appl. Supercond.*, vol. 25, no. 3, pp. 1–4, Jun. 2015.

[30] L. Hao, J. Gallop, D. Cox, and J. Chen, "Fabrication and Analogue Applications of NanoSQUIDs Using Dayem Bridge Junctions," *IEEE J. Sel. Top. Quantum Electron.*, vol. 21, no. 2, pp. 1–8, Mar. 2015.

[31] I. Al-Mashhadani and S. Hadjiloucas, "Linearized Bond Graph of Hodgkin-Huxley Memristor Neuron Model," in *CNNA 2016*, 2016.